Electron-Transfer-Mediated Decay and Interatomic Coulombic Decay from the Triply Ionized States in Argon Dimers

K. Sakai,[1] S. Stoychev,[2] T. Ouchi,[1] I. Higuchi,[3] M. Schöffler,[4] T. Mazza,[1,5] H. Fukuzawa,[1] K. Nagaya,[6] M. Yao,[6] Y. Tamenori,[3] A. I. Kuleff,[2] N. Saito,[7] and K. Ueda[1,*]

[1]*Institute of Multidisciplinary Research for Advanced Materials, Tohoku University, Sendai 980-8577, Japan*
[2]*Theoretische Chemie, PCI, Universität Heidelberg, D-69120 Heidelberg, Germany*
[3]*Japan Synchrotron Radiation Research Institute, Sayo, Hyogo 679-5198, Japan*
[4]*Chemical Sciences Division, Lawrence Berkeley National Laboratory, Berkeley, California 94720, USA*
[5]*Cimaina and Dipartimento di Fisica, Università degli Studi di Milano, via Celoria 16 20133 Milano, Italy*
[6]*Department of Physics, Kyoto University, 606-8502 Kyoto, Japan*
[7]*National Institute of Advanced Industrial Science and Technology, NMIJ, Tsukuba 305-8568, Japan*

(Received 6 October 2010; published 18 January 2011)

We report the first observation of electron-transfer-mediated decay (ETMD) and interatomic Coulombic decay (ICD) from the triply charged states with an inner-valence vacancy, using the Ar dimer as an example. These ETMD and ICD processes, which lead to fragmentation of Ar^{3+}-Ar into Ar^{2+}-Ar^{2+} and Ar^{3+}-Ar^{+}, respectively, are unambiguously identified by electron-ion-ion coincidence spectroscopy in which the kinetic energy of the ETMD or ICD electron and the kinetic energy release between the two fragment ions are measured in coincidence.

DOI: 10.1103/PhysRevLett.106.033401 PACS numbers: 36.40.Mr, 33.80.Eh, 79.60.Jv

Inner-shell vacancy states of isolated atoms and molecules with energies above the double ionization threshold may be subject to electronic decay by electron emission. This process is known as Auger decay [1]. Auger decay has intrinsically intra-atomic nature. In molecular Auger decay, the Auger spectra can be viewed as fingerprint images of the atom where the inner-shell vacancy is created [2]. More than a decade ago, Cederbaum *et al.* [3] predicted a new mechanism of electronic decay where the environment plays a role. For isolated atoms or molecules with an inner-valence vacancy, Auger decay is usually energetically forbidden, but interatomic or intermolecular Coulombic decay (ICD) may occur when another atom or molecule is in close proximity. Marburger *et al.* [4] were the first who observed the ICD in 2*s* ionized Ne clusters. Jahnke *et al.* [5] reported clear experimental evidence for ICD in 2*s* ionized Ne dimers (Ne_2) using cold-target recoil ion momentum spectroscopy, also called reaction microscope [6]. The initial states of ICD can be not only inner-valence ionized states [3–5,7] but also resonant neutral states [8], ionic satellite states [9], and Auger final dicationic states [10,11]. ICD occurs in van der Waals clusters and condensed matters [4,5,7,12] as well as in hydrogen-bonded clusters and solutions [3,13–16]. ICD appears everywhere and plays a key role to transfer the charge and energy between the concerned atom or molecule and its environment. It is pointed out also that low-energy electron generation via ICD in the aqueous environment may be relevant to radiation damage in biological matter [14–16]. It is worth noting that ICD in highly (e.g., triply) charged species with a neighbor has never been investigated in spite of the vast amount of the ICD works described above.

From the theoretical point of view, ICD is driven by the Coulomb interaction described by the two-electron integral, as is the case for the Auger decay. The low-energy electron with a large de Broglie wavelength is characteristic to ICD emission and connects two outer-valence orbitals located at two distant atoms or molecules. Let us consider the ICD in a van der Waals dimer *AB* illustrated in Fig. 1 as the simplest example. An atom *A* with an inner-valence vacancy transfers its energy to a neighboring atom *B* which subsequently releases its energy by emitting an electron from its outer-valence orbital [Fig. 1(a)]. This energy transfer process corresponds to the direct Coulomb term of the two-electron integral. This term causes an asymptotic behavior of the ICD rate of R^{-6} (R being the internuclear distance) characteristic of dipole-dipole interaction and thus can be viewed as virtual photon exchange [17]. The ICD rate caused by the exchange term [Fig. 1(b)], on the other hand, drops exponentially as a function of R. The exchange ICD leads to final states that are different from those of direct ICD, due to symmetry reasons [18]. The exchange ICD is usually much weaker than the direct ICD but becomes dominant if the

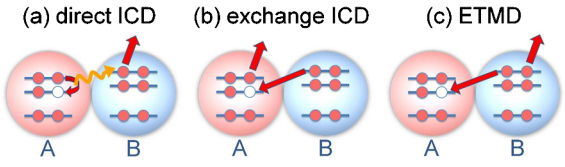

FIG. 1 (color online). Schematic diagrams of (a) direct ICD (interatomic Coulombic decay), (b) exchange ICD, and (c) ETMD (electron-transfer-mediated decay).

direct ICD is energetically closed [18]. There is another class of ICD-related processes, as illustrated by Fig. 1(c), where the outer-valence electron of the neighboring atom B fills the inner-valence vacancy of atom A and another outer-valence electron of the atom B is emitted. This process is called electron-transfer-mediated decay (ETMD) [19]. ETMD is different from ICD in the final charge states of both atoms. In ETMD, the charge state of the atom A that had the initial vacancy decreases by one while the originally neutral neighboring atom B now becomes doubly charged. Though ETMD was theoretically predicted a decade ago [19], there has been no conclusive experimental evidence reported so far.

In the present work, we have investigated ICD and ETMD from the triply charged state with an inner-valence $3s$ vacancy $Ar^{3+}(3s3p^4)$-Ar. The channels we focused on were the Coulomb breakup of $Ar^{3+}(3p^3)$-$Ar^{+}(3p^5)$ populated by ICD and $Ar^{2+}(3p^4)$-$Ar^{2+}(3p^4)$ populated by ETMD. We detected slow electrons in coincidence with these two ion pairs using momentum-resolved electron-ion-ion coincidence spectroscopy (equivalent to cold-target recoil ion momentum spectroscopy or reaction microscope) and extracted the correlation between the kinetic energy of the ICD and ETMD electrons and kinetic energy release (KER), i.e., the sum of the energies of the two ions.

The experiment was carried out on the c branch of the beam line 27SU [20] at SPring-8. The storage ring was operated in several-bunches mode providing 53 single bunches (4/58 filling bunches) separated by 82.6 ns. The argon dimers were produced by the expansion of argon gas at 300 K at a stagnation pressure of ~0.5 MPa, through a pinhole of 80 μm diameter. The cluster beam was directed vertically, parallel to the orientation of the E vector of the incident linearly polarized light. Our momentum-resolved electron-ion-ion coincidence spectroscopy is based on recording the electron and ion times-of-flight (TOFs) with position and time-sensitive multihit-capable detectors (Roentdek HEX120 for electrons and HEX80 for ions). Knowledge of position and arrival time on the particle detectors, (x, y, t), allows us to extract information about the 3D momentum of each particle. The electron and ion TOF spectrometers were placed face to face. The TOF spectrometer axis was horizontal and perpendicular to both the photon beam and the cluster beam. Detailed description and typical operation conditions of the spectrometers were described elsewhere [21]. The electrons and ions TOFs were recorded with respect to the bunch marker of the light source using multihit time-to-digital converters (Roentdek TDC8HP), selecting only electron signals synchronized with the single bunches by logic gating. The measurements were carried out at a photon energy of 345.5 eV.

Figure 2 shows the ion-ion coincidence TOF spectrum. The x and y coordinates correspond to the TOFs of the first and the second ions of the coincidence pair. Only the ion pairs satisfying the momentum conservation laws within the plane perpendicular to the TOF axis are plotted. The results shown below are further filtered by the momentum conservation parallel to the TOF axis and thus by suppression of the false coincidences in Fig. 2. The ion pair Ar^{+}-Ar^{+} is formed mostly as a result of radiative charge transfer from the $Ar^{2+}(3p^4)$-Ar states [22]. The ion pair Ar^{2+}-Ar^{+} is mostly formed as a result of ICD from the satellite states $Ar^{2+}(3p^3 3d)$-Ar [11]. The ion pairs Ar^{3+}-Ar^{+} and Ar^{2+}-Ar^{2+} are the ones we focus on. The sum of the counts for the Ar^{3+}-Ar^{+} and Ar^{2+}-Ar^{2+} pairs is 0.4 ± 0.1 times the counts for the Ar^{2+}-Ar^{+} pair, while the counts for Ar^{4+} originating from free atoms are by an order smaller than those of Ar^{3+}. These observations indicate that the production of the quadruply charged states Ar^{3+}-Ar^{+} and Ar^{2+}-Ar^{2+} are enhanced in the dimer relative to the corresponding Ar^{4+} states in the free atom. Hence, they imply that Ar^{3+}-Ar^{+} and Ar^{2+}-Ar^{2+} are produced not only via charge redistribution from the quadruply charged states Ar^{4+}-Ar but also via interatomic electronic decay from the triply charged states Ar^{3+}-Ar. Referring to Fig. 1, we note again that in ICD the atom with the initial vacancy remains in the same charge state and the neighboring atom is singly ionized, and that in ETMD the charge of the atom with the initial vacancy decreases by one and the neighboring atom is doubly ionized. Thus, it is well expected that Ar^{3+}-Ar^{+} and Ar^{2+}-Ar^{2+} are formed as results of ICD and ETMD, respectively, from the triply charged states Ar^{3+}-Ar.

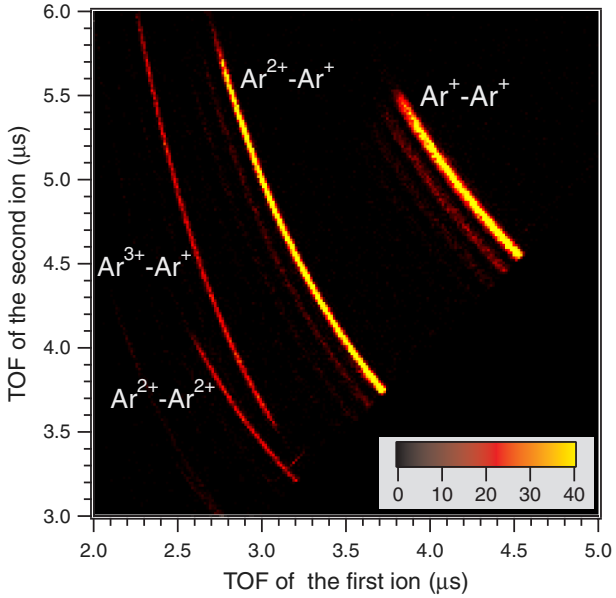

FIG. 2 (color online). Ar dimer ion-ion coincidence TOF spectrum.

The relationship between the electron energy and the KER in the fragmentation into Ar^{3+}-Ar^{+} is shown in Fig. 3(a). The Ar^{3+}-Ar^{+} pair is formed via ICD from Ar^{3+}-Ar created by single-photon triple ionization of the

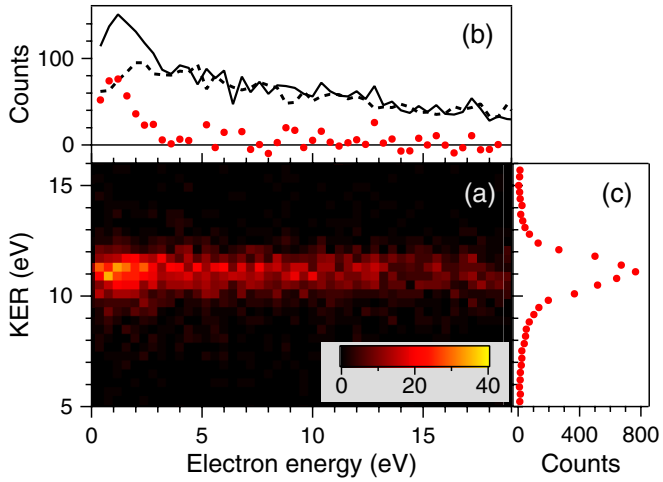

FIG. 3 (color online). (a) Relationship between the ICD electron energy and the total KER for the Ar^{3+}-Ar^{+} fragmentation of the argon dimer. (b) Kinetic energy distribution of the ICD electrons detected in coincidence with Ar^{3+}-Ar^{+} pairs.

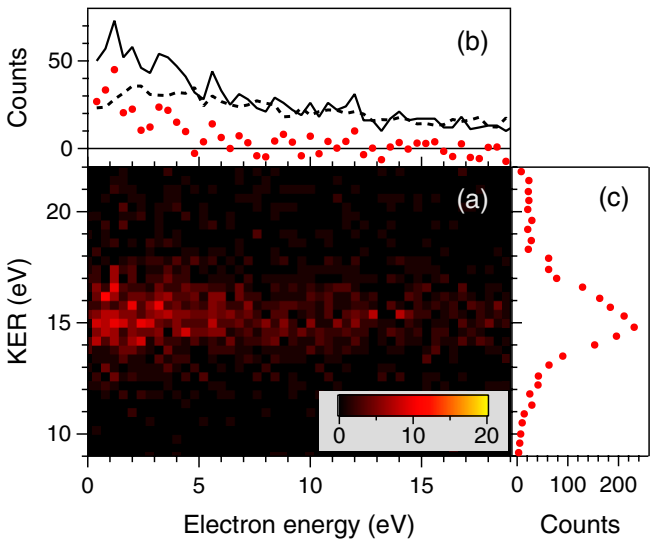

FIG. 4 (color online). Relationship between the ETMD electron energy and the total KER for the Ar^{2+}-Ar^{2+} fragmentation of the argon dimer. See the caption of Fig. 3 for the details.

argon dimer. Single-photon triple ionization may be caused by sequential Auger transitions following Ar $2s$ photoionization, double Auger transitions following Ar $2p$ photoionization, and direct triple photoionization. These branching ratios cannot be obtained from the present results. In Fig. 3(b), the energy distribution of electrons recorded in coincidence with Ar^{3+}-Ar^{+} ion pairs and in coincidence with Ar^{+}-Ar^{+} ion pairs are given by the solid line and the dashed line, respectively. The latter is scaled to match the former at high energy. The latter gives the background coming from the false coincidences because the true electron signals in coincidence with Ar^{+}-Ar^{+} ion pairs are expected to be zero in this energy region [23]. The result of the background subtraction is given by the dots. The energy distribution of the ICD electrons thus obtained exhibits a peak at ~1 eV. Figure 3(c) shows the distribution of the KER between Ar^{3+}-Ar^{+} from the Ar dimer. The peak energy is 11 eV, which coincides with the Coulomb repulsion energy calculated from the bond length of the neutral Ar dimer 3.76 Å [24], implying that ICD occurs without much nuclear dynamics.

The relationship between the electron energy and the KER in the fragmentation into Ar^{2+}-Ar^{2+} is shown in Fig. 4(a). As discussed above, the Ar^{2+}-Ar^{2+} pair can be formed via ETMD from Ar^{3+}-Ar. Figure 4(b) shows the energy distribution of the ETMD electrons in coincidence with Ar^{2+}-Ar^{2+}. Though the statistics is rather poor after the background subtraction, it is clear that the ETMD electron signal decreases sharply with the increase in energy. Figure 4(c) shows the KER distribution. The peak energy of ~15 eV again corresponds to the Coulomb repulsion energy at the bond length of the neutral Ar dimer 3.76 Å.

Figure 5 is a schematic energy diagram for the initial and final states of ICD and ETMD. Energies of the initial states Ar^{3+}-Ar (labeled by Arabic numbers 1–10) are approximated by the horizontal lines given by the relevant atomic energies [25]. Energies of the final states Ar^{3+}-Ar^{+} (labeled by letters *A*-*C*) and Ar^{2+}-Ar^{2+} (*D*-*I*) are approximated by the sum of the atomic energies [25] and Coulomb repulsion energies. Let us focus on the initial states with the inner-valence $3s$ vacancy (thick lines 5, 7, 9, 10). These states are mostly below the ICD final states Ar^{3+}-Ar^{+} (*A*-*C*) in the Franck-Condon region (~ 3.76 Å). Only one ICD channel from $Ar^{3+}(3s3p^4\,{}^2P)$-Ar (line 5) to $Ar^{3+}(3p^3\,{}^4S)$-$Ar^{+}(3p^5\,{}^2P)$ (line *C*) is energetically allowed. This ICD is the exchange ICD [Fig. 1(b)] because the spin is flipped in the atom with the initial $3s$ vacancy [18]. The expected kinetic energy of the ICD electrons is ~1 eV, in reasonable agreement with the observation in Fig. 3. The next two $3s$ vacancy states $Ar^{3+}(3s3p^4\,{}^2S)$-Ar (line 7) and $Ar^{3+}(3s3p^4\,{}^2D)$-Ar (line 9) are not subject to ICD but can lead to the states Ar^{2+}-Ar^{2+} below them via ETMD. The lowest $3s$ vacancy state $Ar^{3+}(3s3p^4\,{}^4P)$-Ar is subject to neither ICD nor ETMD since they are energetically forbidden.

There are satellite states $Ar^{3+}(3p^2 4s, 3d)$-Ar that may be the initial states of ICD and ETMD in the relevant energy region and some of them are also included in Fig. 5 (thin dashed lines). The states $Ar^{3+}(3p^2 4s\,{}^2D, {}^2P)$-Ar (lines 1, 2) are subject to direct ICD to $Ar^{3+}(3p^3\,{}^2P, {}^2D)$-$Ar^{+}(3p^5\,{}^2P)$ (lines *A*, *B*). The states $Ar^{3+}(3p^2 3d\,{}^2D)$-Ar (line 4) and $Ar^{3+}(3p^2 3d\,{}^4P)$-Ar (line 6) are also subject to direct ICD to $Ar^{3+}(3p^3\,{}^2D)$-$Ar^{+}(3p^5\,{}^2P)$ (line *B*) and $Ar^{3+}(3p^3\,{}^4S)$-$Ar^{+}(3p^5\,{}^2P)$ (line *C*), respectively. There are ETMD channels that are open from the satellite state $Ar^{3+}(3p^2 3d\,{}^2P)$-Ar (line 8) to $Ar^{2+}(3p^4)$-$Ar^{2+}(3p^4)$ (say, lines *G*-*H*). These ETMDs

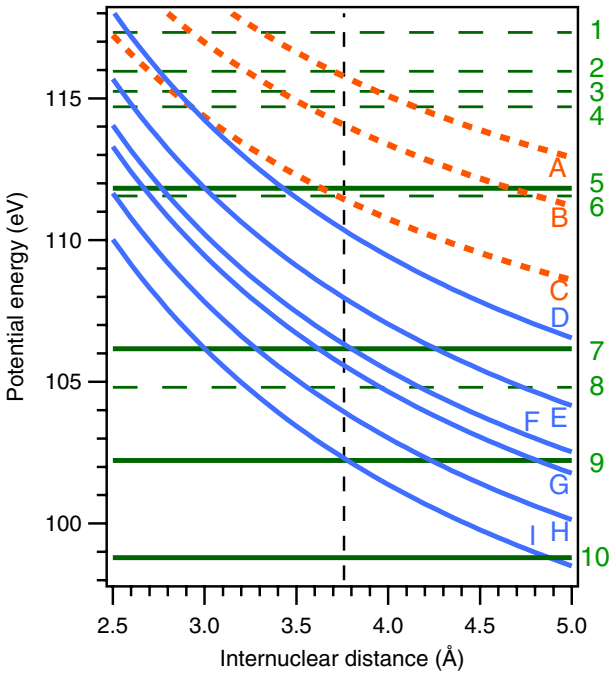

FIG. 5 (color online). Schematic energy diagram for the initial (labeled by 1–10) and final (labeled by *A-C* for ICD and *D-I* for ETMD) states of the interatomic processes. Initial states decay to final states which are energetically below them. 1, $Ar^{3+}(3p^2(^1D)4s\,^2D)$-Ar; 2, $Ar^{3+}(3p^2(^3P)4s\,^2P)$-Ar; 3, $Ar^{3+}(3p^2(^3P)4s\,^4P)$-Ar; 4, $Ar^{3+}(3p^2(^1D)3d\,^2D)$-Ar; 5, $Ar^{3+}(3s3p^4\,^2P)$-Ar; 6, $Ar^{3+}(3p^2(^3P)3d\,^4P)$-Ar; 7, $Ar^{3+}(3s3p^4\,^2S)$-Ar; 8, $Ar^{3+}(3p^2(^3P)3d\,^2P)$-Ar; 9, $Ar^{3+}(3s3p^4\,^2D)$-Ar; 10, $Ar^{3+}(3s3p^4\,^4P)$-Ar. A, $Ar^{3+}(3p^3\,^2P)$-$Ar^{+}(3p^5\,^2P)$; B, $Ar^{3+}(3p^3\,^2D)$-$Ar^{+}(3p^5\,^2P)$; C, $Ar^{3+}(3p^3\,^4S)$-$Ar^{+}(3p^5\,^2P)$; D, $Ar^{2+}(3p^4\,^1S)$-$Ar^{2+}(3p^4\,^1S)$; E, $Ar^{2+}(3p^4\,^1D)$-$Ar^{2+}(3p^4\,^1S)$; F, $Ar^{2+}(3p^4\,^3P)$-$Ar^{2+}(3p^4\,^1S)$; G, $Ar^{2+}(3p^4\,^1D)$-$Ar^{2+}(3p^4\,^1D)$; H, $Ar^{2+}(3p^4\,^3P)$-$Ar^{2+}(3p^4\,^1D)$; and I, $Ar^{2+}(3p^4\,^3P)$-$Ar^{2+}(3p^4\,^3P)$. The vertical dashed line corresponds to the equilibrium bond length of the neutral Ar dimer 3.76 Å [24].

are expected to occur as results of configuration mixing between $3s3p^4\,^2P$ and $3s^23p^23d\,^2P$.

In conclusion, we have unambiguously identified ICD and ETMD processes from the triply charged states in the Ar dimer using electron-ion-ion coincidence spectroscopy in which the kinetic energy of the ICD or ETMD electron and the kinetic energy release between the two fragment ions are measured in coincidence, and provided the first unambiguous experimental evidence for ETMD, as well as the first evidence for ICD from multiply charged species with a neighbor.

The experiments were performed at SPring-8 with the approval of JASRI. We are grateful to L. S. Cederbaum for stimulating discussion. The work was supported by Grant-in-Aid for Scientific Research from JSPS, by the Management Expenses Grants for National Universities Corporations from MEXT, and IMRAM research program. M. S. acknowledges the support by the Alexander von Humboldt foundation. A. I. K. acknowledges the support of the European Community's FP7 / ERC Advanced Investigator Grant No. 227597.

Note added.—The ETMD in singly ionized ArKr mixed clusters has been very recently independently observed [26].

*ueda@tagen.tohoku.ac.jp

[1] M. Thompson *et al.*, *Auger Electron Spectroscopy* (Wiley, New York, 1985).
[2] F. Tarantelli and L. S. Cederbaum, Phys. Rev. Lett. **71**, 649 (1993).
[3] L. S. Cederbaum, J. Zobeley, and F. Tarantelli, Phys. Rev. Lett. **79**, 4778 (1997).
[4] S. Marburger, O. Kugeler, U. Hergenhahn, and T. Möller, Phys. Rev. Lett. **90**, 203401 (2003).
[5] T. Jahnke *et al.*, Phys. Rev. Lett. **93**, 163401 (2004).
[6] J. Ullrich *et al.*, Rep. Prog. Phys. **66**, 1463 (2003).
[7] R. Santra, J. Zobeley, L. S. Cederbaum, and N. Moiseyev, Phys. Rev. Lett. **85**, 4490 (2000).
[8] T. Aoto *et al.*, Phys. Rev. Lett. **97**, 243401 (2006).
[9] T. Jahnke *et al.*, Phys. Rev. Lett. **99**, 153401 (2007).
[10] R. Santra and L. S. Cederbaum, Phys. Rev. Lett. **90**, 153401 (2003); **94**, 199901(E) (2005).
[11] Y. Morishita *et al.*, Phys. Rev. Lett. **96**, 243402 (2006).
[12] R. Santra, J. Zobeley, and L. S. Cederbaum, Phys. Rev. B **64**, 245104 (2001).
[13] E. F. Aziz *et al.*, Nature (London) **455**, 89 (2008).
[14] T. Jahnke *et al.*, Nature Phys. **6**, 139 (2010).
[15] M. Mucke *et al.*, Nature Phys. **6**, 143 (2010).
[16] O. Vendrell, S. D. Stoychev, and L. S. Cederbaum, Chem. Phys. Chem. **11**, 1006 (2010).
[17] R. Santra and L. S. Cederbaum, Phys. Rep. **368**, 1 (2002).
[18] K. Kreidi *et al.*, J. Phys. B **41**, 101002 (2008).
[19] J. Zobeley, R. Santra, and L. S. Cederbaum, J. Chem. Phys. **115**, 5076 (2001).
[20] H. Ohashi *et al.*, Nucl. Instrum. Methods Phys. Res., Sect. A **467–468**, 529 (2001); **467–468**, 533 (2001).
[21] K. Ueda *et al.*, J. Electron Spectrosc. Relat. Phenom. **166–167**, 3 (2008).
[22] N. Saito *et al.*, Chem. Phys. Lett. **441**, 16 (2007).
[23] K. Ueda *et al.*, J. Electron Spectrosc. Relat. Phenom. **155**, 113 (2007).
[24] J. F. Ogilvie and F. Y. H. Wang, J. Mol. Struct. **273**, 277 (1992).
[25] http://physics.nist.gov/PhysRefData/ASD/levels_form.html.
[26] M. Förstel, M. Mucke, T. Arion, A. M. Bradshaw, and U. Hergenhahn, Phys. Rev. Lett. **106**, 033402 (2011).